CONTROL ALLOCATION: ENHANCING THE PERFORMANCE OF QUADROTORS HIGH-LEVEL CONTROLLERS

João C. Monteiro*, Fernando Lizarralde*, Liu Hsu*

*Dept. of Electrical Eng., COPPE/Federal University of Rio de Janeiro, Rio de Janeiro, Brazil

Emails: jcmonteiro@poli.ufrj.br, [fernando, liu]@coep.ufrj.br

Abstract— This paper studies four control allocations strategies with applications to quadrotor unmanned aerial vehicles (UAVs). Control allocation determines how a desired control effort is distributed among the available system inputs. When a system has more actuators than task degrees of freedom (DoF), this problem poses itself naturally, since there are multiple actuators choices capable of generating the same control effort. On the other hand, if the task DoF equals the number of actuators, unless some sort of saturation occurs, the mapping between control effort and actuators inputs is unique. This is exactly the case for quadrotor UAVs. To countermeasure this input saturation, four control allocation strategies are presented. The first is derived from the well known weighted least squares (WLS) criterion optimization. To obtain a more predictable control degradation, the direct control allocation (DCA) is introduced. Then, a generalization of the DCA, called partial control allocation (PCA) is studied. The last studied control allocation strategy is a suboptimal variation of the PCA (S-PCA). Simulations of the last three methods are conducted and their performance is compared.

Keywords— Control Allocation, Quadrotor, UAV.

Resumo— Este artigo estuda quatro estratégias de distribuição de controle com aplicações a veículos aéreos não-tripulados (VANTs) quadrirrotores. A distribuição de controle determina como um esforço de controle desejado é distribuído entre as entradas disponíveis de um sistema. Quando um sistema possui mais atuadores do que graus de liberdade (DoF) da tarefa, este problema surge naturalmente, dado que há múltiplas escolhas de atuadores que produzem o mesmo esforço de controle. Em contrapartida, se a tarefa possui DoF igual à quantidade de atuadores, a menos que ocorra saturação, o mapeamento entre esforços de controle e ação dos atuadores é único. Este é exatamente o caso para quadrirrotores. Para combater esta saturação de entrada, quatro estratégias de distribuição de controle são apresentadas. A primeira deriva diretamente da otimização do critério de mínimos quadrados ponderado (WLS). Visando obter uma degradação mais previsível do controle, o método de alocação direta (DCA) é introduzido. Em seguida, uma generalização do método, denominada PCA é estudada. A última estratégia de distribuição estudada é uma variação subótima do PCA (S-PCA). Simulações dos últimos três métodos são conduzidas e o desempenho dos algoritmos é comparado.

Palavras-chave— Distribuição de Controle, Quadrirrotor, VANT.

1 Introduction

Control allocation determines how to share the control demand between the multiple actuator systems. Since control allocation acts on a given control input, this stage can be treated independently of the high-level motion controllers design. This separation is advantageous because both motion control stages, i.e. high-level control and control allocation, can be improved individually and then combined to enhance system performance.

When a system possesses multiple control inputs, the problem of control allocation appears naturally. This happens because there are multiple actuators configurations that produce the same control effort. This characterizes a redundant control allocation problem, as stated by Ducard and Hua (2011), and is the case for multirotors with more than four propellers. For these redundant systems, there are several control allocation strategies present in the literature (Johansen and Fossen, 2013), such as linear and quadratic programming, multi-saturation anti-windup, and model predictive control. Regarding quadrotor UAVs, most of the research is directed towards fault tolerant systems (Marks et al., 2012; Yoon et al., 2016), where the objective is to redistribute the demand due to the fault or loss of one or more propulsion groups. In contrast, we study the effects of actuator saturation on control allocation of quadrotors, and how optimization may be used to choose the best possible control vector.

In this paper the results presented by Monteiro et al. (2016) are extended, and the pros and cons of each control allocation strategy are discussed based on a simulated flight scenario. Assuming that saturation occurs and the prescribed control demand cannot be met, four distinct control allocation methods are studied[1]. The first attempt aims at minimizing a weighted quadratic criterion, reformulated as a QP problem. This reformulation could reduce computational cost and allow real-time implementation of the algorithm, which is desirable for embedded systems. However, this solution does not guarantee that the generated efforts and the desired ones point in the same direction. To solve this issue, the direct control allocation (DCA), a method that searches for vectors that keep the desired control direction is studied, and a simple closed solution is found. It is

[1]If one considers that allowing the motors to saturate arbitrarily also characterizes control allocation, then there are actually five studied strategies.

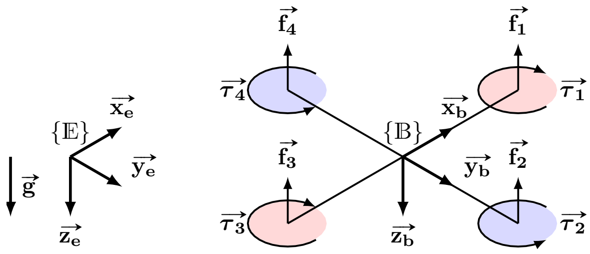

Figure 1: Free body diagram of a quadrotor with propellers arranged symmetrically around the center of mass, main propellers efforts, a body fixed frame $\{\mathbb{B}\}$, and an inertial frame $\{\mathbb{E}\}$.

shown that this solution might not exist, and does not ensure maximum attainable torque. These points lead to the partial control allocation (PCA) strategy, and the further development of the S-PCA, a suboptimal variation of the last. Finally, the last three strategies are evaluated in a rapid ascent flight simulation.

2 Problem Formulation

2.1 Rigid Body Dynamics

Consider a quadrotor with four propellers, as shown in Figure 1. Each propeller generates a torque $\vec{\tau_i}$ on the body, about its $\vec{z_b}$ axis, that opposes the propeller rotation. The propellers also generate forces $\vec{f_i}$ on the body, along its $\vec{z_b}$ axis. The rotation from $\{\mathbb{E}\}$ to $\{\mathbb{B}\}$ is denoted by $\mathbf{R} \in \mathrm{SO}(3)$.

The position of the quadrotor center of mass, expressed in an inertial frame, is $\mathbf{p} \in \mathbb{R}^3$. Then, the quadrotor translational dynamics are

$$m\ddot{\mathbf{p}} = mg\mathbf{z} - \mathbf{R}\mathbf{z}\sum_{i=1}^{4} f_i \ , \tag{1}$$

where m is the vehicle mass, g the gravity magnitude, and $\mathbf{z} = [0\ 0\ 1]^{\mathrm{T}}$. Expressed in $\{\mathbb{B}\}$, the body angular velocity w.r.t. $\{\mathbb{E}\}$ is $\boldsymbol{\omega} \in \mathbb{R}^3$, and it is governed by the dynamic equation

$$\mathbf{J}\dot{\boldsymbol{\omega}} + \boldsymbol{\omega} \times \mathbf{J}\boldsymbol{\omega} = \begin{bmatrix} l\,(f_4 - f_2) \\ l\,(f_1 - f_3) \\ (\tau_2 - \tau_1 + \tau_4 - \tau_3) \end{bmatrix}, \tag{2}$$

where l is the distance from the body center of mass to the propellers, and $\mathbf{J} \in \mathbb{R}^{3\times3}$ the body inertia matrix.

As discussed in (Bouabdallah, 2007), since the propellers direction of rotation does not change, the forces and torques generated by the propulsion groups are written in terms of the propellers velocities v_i squared, such as[2]:

$$f_i = \kappa_t v_i^2, \tag{3}$$
$$\tau_i = \kappa_d v_i^2, \tag{4}$$

[2]If the propellers are allowed to change the rotation direction, the term v_i^2 is changed to $|v_i|\, v_i$.

where $\kappa_t > 0$ is the rotor thrust coefficient and $\kappa_d > 0$ the rotor drag coefficient. From (3) and (4) linear mapping from the vector of quadratic rotor speeds $\mathbf{v} \in \mathbb{R}^4$ and the vector of control efforts $\mathbf{u} \in \mathbb{R}^4$ is written. This mapping is characterized by the decoupling matrix $\mathbf{M} \in \mathbb{R}^{4\times4}$,

$$\underbrace{\begin{bmatrix} u_1 \\ u_2 \\ u_3 \\ u_4 \end{bmatrix}}_{\mathbf{u}} = \underbrace{\begin{bmatrix} \kappa_t & \kappa_t & \kappa_t & \kappa_t \\ 0 & -l\kappa_t & 0 & l\kappa_t \\ l\kappa_t & 0 & -l\kappa_t & 0 \\ -\kappa_d & \kappa_d & -\kappa_d & \kappa_d \end{bmatrix}}_{\mathbf{M}} \underbrace{\begin{bmatrix} v_1^2 \\ v_2^2 \\ v_3^2 \\ v_4^2 \end{bmatrix}}_{\mathbf{v}} . \tag{5}$$

Then, the equations of motion are rewritten as

$$m\ddot{\mathbf{p}} = mg\mathbf{z} - u_1\mathbf{R}\mathbf{z} \ , \tag{6}$$
$$\mathbf{J}\dot{\boldsymbol{\omega}} = u_2\mathbf{x} + u_3\mathbf{y} + u_4\mathbf{z} - \boldsymbol{\omega} \times \mathbf{J}\boldsymbol{\omega} \ . \tag{7}$$

Remark. From (5) it is clear that control allocation is not affected by possible changes in the model, as previously stated.

2.2 Control Allocation Model

Note that the components u_1 and $u_{2,3,4}$ represent a force along $\vec{z_b}$ and torques about $\vec{x_b}$, $\vec{y_b}$, and $\vec{z_b}$, respectively. Consequently, $\mathbf{u}$ is the vector of control efforts. High-level control strategies are synthesized from (6) and (7), using $\mathbf{u}$ as the control input, see (Bouabdallah, 2007; Mellinger and Kumar, 2011; Mellinger et al., 2012). These controllers produce a desired control vector $\mathbf{u_d}$.

The inverse mapping, that produces the propeller velocities from the efforts, is

$$\underbrace{\begin{bmatrix} v_1^2 \\ v_2^2 \\ v_3^2 \\ v_4^2 \end{bmatrix}}_{\mathbf{v}} = \underbrace{\frac{1}{4l\kappa_t}\begin{bmatrix} l & 0 & 2 & -l\kappa_t\kappa_d^{-1} \\ l & -2 & 0 & l\kappa_t\kappa_d^{-1} \\ l & 0 & -2 & -l\kappa_t\kappa_d^{-1} \\ l & 2 & 0 & l\kappa_t\kappa_d^{-1} \end{bmatrix}}_{\mathbf{M^{-1}}} \underbrace{\begin{bmatrix} u_1 \\ u_2 \\ u_3 \\ u_4 \end{bmatrix}}_{\mathbf{u}} . \tag{8}$$

Although this matrix is invertible, the inverse mapping might produce an unreachable velocity vector $\mathbf{v}$. This is because actuators are subject to bound constraints. Therefore, the control allocation of a quadrotor UAV is formulated as follows:

Find $\mathbf{v}$ *from* (8)*, subject to*

$$0 \le v_{\min}^2 \le v_i^2 \le v_{\max}^2, \ \forall i, \tag{9}$$

that best meets the desired control vector $\mathbf{u_d}$.

Inequality (9) defines a feasible set $\mathbb{W}$. Naturally, if the value obtained when $\mathbf{u_d}$ is applied to (8) lies inside $\mathbb{W}$, the solution is trivial. Furthermore, (5) maps $\mathbb{W}$ into a feasible set of control efforts $\mathbb{U}$. Hence, if $\mathbf{u_d} \in \mathbb{U}$ the solution is also straightforward.

In general, the boundary $\partial\mathbb{U}$ of the feasible set $\mathbb{U}$ is obtained from $\partial\mathbb{W}$, but it may not be

ISSN 2525-8311

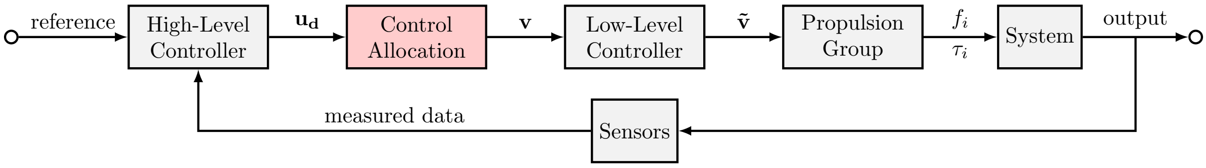

Figure 2: Basic motion control structure of a quadrotor, where the control allocation step is highlighted. The vector $\tilde{\mathbf{v}}$ is the actual physical signal that commands the propulsion group.

the image of $\partial\mathbb{W}$ (Durham, 1993). This happens when points on $\partial\mathbb{W}$ are mapped into the interior of $\mathbb{U}$. Nonetheless, since the mapping is a homeomorphism, $\partial\mathbb{U}$ is a simple image of $\partial\mathbb{W}$, obtained from (5) (Monteiro et al., 2016).

The basic motion control scheme of a quadrotor UAV is depicted in Figure 2.

3 Control Allocation

3.1 Quadratic Programming (QP)

Assuming the desired control vector violates (9), it needs to be adjusted. Ideally, this choice should follow some optimization criterion. The weighted least squares (WLS) is a good first attempt in this direction, as it finds $\mathbf{u}$ that minimizes the distance between $\mathbf{u_d}$ and $\mathbf{u}$.

Then, consider the following WLS constrained optimization problem to find the control $\mathbf{u}$:

$$\begin{aligned} &\min : \|\mathbf{W}(\mathbf{u}-\mathbf{u_d})\|_2^2 \,, \\ &\text{s.t.} : \underbrace{\begin{bmatrix} \mathbf{I} \\ -\mathbf{I} \end{bmatrix}}_{\mathbf{A}} \mathbf{v} = \mathbf{A}\mathbf{M}^{-1}\mathbf{u} \le \underbrace{\begin{bmatrix} v_{\max}^2 \mathbf{1} \\ -v_{\min}^2 \mathbf{1} \end{bmatrix}}_{\mathbf{b}}, \end{aligned} \tag{10}$$

where $\mathbf{W} \in \mathbb{R}^{4\times 4}$ is a weighting matrix with full rank, $\mathbf{I} \in \mathbb{R}^{4\times 4}$ an identity matrix, and $\mathbf{1} \in \mathbb{R}^4$ a vector of ones. This equation can be readily rewritten in the usual QP format:

$$\begin{aligned} &\min : \bar{\mathbf{u}}^{\mathrm{T}}\mathbf{Q_u}\bar{\mathbf{u}}, \\ &\text{s.t.} : \bar{\mathbf{A}}\bar{\mathbf{u}} \le \bar{\mathbf{b}}, \end{aligned} \tag{11}$$

with $\mathbf{Q_u} = \mathbf{W}^{\mathrm{T}}\mathbf{W}$, $\bar{\mathbf{A}} = \mathbf{A}\mathbf{M}^{-1}$, $\bar{\mathbf{b}} = \mathbf{b} - \bar{\mathbf{A}}\mathbf{u_d}$, and $\bar{\mathbf{u}} = \mathbf{u} - \mathbf{u_d}$.

The constrains posed by equation (11) define a convex polytope. However, QP solvers perform better with bound constraints. Therefore, from (5), (8) and (9) the optimization is reformulated for $\mathbf{v}$ as:

$$\begin{aligned} &\min : \bar{\mathbf{v}}^{\mathrm{T}}\mathbf{Q_v}\bar{\mathbf{v}}, \\ &\text{s.t.} : v_{\min}^2 - (\mathbf{v_d})_i \le (\bar{\mathbf{v}})_i \le v_{\max}^2 - (\mathbf{v_d})_i, \end{aligned} \tag{12}$$

with $\mathbf{Q_v} = (\mathbf{WM})^{\mathrm{T}}(\mathbf{WM})$, $\bar{\mathbf{v}} = \mathbf{v} - \mathbf{v_d}$, $\mathbf{v_d} = \mathbf{M}^{-1}\mathbf{u_d}$, and $(\mathbf{x})_i$ denoting the i-th component of the vector $\mathbf{x}$.

To solve (12) there are very efficient QP solvers there are suitable for real-time implementation. For instance, Petersen and Bodson (2006) propose active set algorithms, and Härkegård (2002) propose an interior point algorithm.

3.2 Direct Control Allocation (DCA)

Instead of finding a vector that minimizes the l_2 distance, a solution that is very common in flight control applications is the direct control allocation (DCA) (Durham, 1993). The DCA objective is to keep the direction of the desired control vector, while allocating a feasible control vector. For a mapping such as (5) and (8), the following steps describe the DCA method:

1. Find $\alpha \in \mathbb{R}$ that solves the following optimization problem:

$$\begin{aligned} \min \; &: \|\mathbf{u_d} - \alpha\mathbf{u_d}\|_2 \,, \\ \text{s.t.} \; &: \begin{matrix} \alpha\mathbf{u_d} \in \mathbb{U} \\ \alpha > 0 \end{matrix} \end{aligned} \tag{13}$$

2. Define the solution $\mathbf{v} = \alpha\mathbf{M}^{-1}\mathbf{u_d}$.

Therefore, if $\mathbf{u_d} \in \mathbb{U}$ it follows that $\alpha = 1$ solves (13) and $\mathbf{v} \in \mathbb{U}_\tau$. Otherwise, the solution is projected onto the nearest point on $\partial\mathbb{U}$ that keeps the direction of $\mathbf{u_d}$. It is worth noting that a solution to (13) may not exist. In such cases, one might use the QP formulation (12), or one of the techniques presented on Sections 3.3 and 3.4.

Solution 1 *Given the desired motors squared velocities* $\mathbf{v_d} \notin \mathbb{U}_\tau$*, the solution of* (13)*, when it exists, is*

$$\alpha = \begin{cases} v_{\max}^2 / \|\mathbf{v_d}\|_\infty & , \|\mathbf{v_d}\|_\infty > v_{\max}^2 \\ v_{\min}^2 / \|\mathbf{v_d}\|_\infty & , \text{otherwise} \end{cases} . \tag{14}$$

Since $\mathbb{W}$ is a hypercube, the proof that α from (14) is such that $\alpha\mathbf{v_d} \in \partial\mathbb{W}$ and $\|\mathbf{v_d} - \alpha\mathbf{v_d}\|_2$ is minimum follows from simple geometry[3]. From (5) and the homeomorphism property, we have that $\alpha\mathbf{u_d} \in \partial\mathbb{U}$ and $\|\mathbf{u_d} - \alpha\mathbf{u_d}\|_2$ is also minimum.

Remark. The DCA solution given in Solution 1 might not be valid. This fact is illustrated in Figure 3, where three different sets are compared. The last two always admit a solution, while the first, which corresponds to the quadrotor DCA problem, does not. Note that even if $v_{\min}^2 = 0$ a solution might no exist depending on the required control direction. This happens because the constraint on α is a strict inequality, cf. (13).

[3]Note that α in (14) is such that the largest (smallest) component of $\mathbf{v_d}$ is saturated to the closest bound

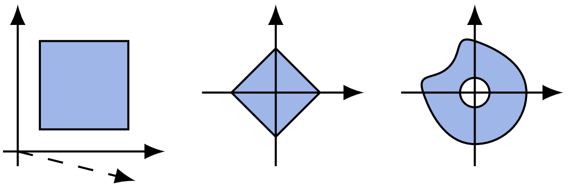

(a) × (b) ✓ (c) ✓

Figure 3: According to the optimization problem posed on (13), sets (b) and (c) admit a solution, while set (a) does not.

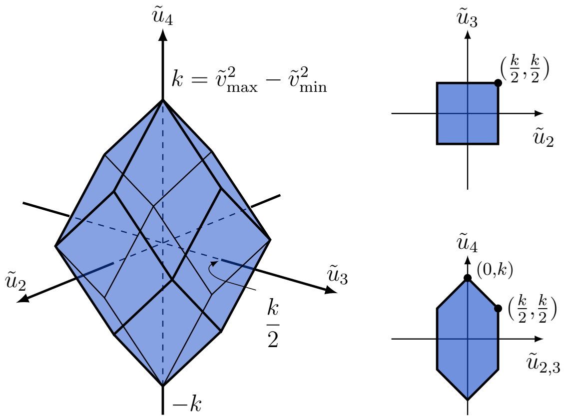

Figure 4: The feasible moments dodecahedron $\mathbb{U}_\tau$. To generate $\mathbb{U}_\tau$, cut a regular octahedron on $\tilde{u}_2 = \pm k/2$ and $\tilde{u}_3 = \pm k/2$.

3.3 Partial Control Allocation (PCA)

The PCA problem (Monteiro et al., 2016) searches for solutions $\mathbf{u} \in \partial\mathbb{U}$ that preserve the direction of some subvector of $\mathbf{u_d}$. For the remaining efforts, another optimization problem is solved if needed.

The underlying motivation for choosing the PCA is to adapt the original objective of the DCA, that is: produce a predictable degradation of forces and moments (Johansen and Fossen, 2013). Instead, one should firstly determine to meet either one, and then optimize the other.

Choosing to partition the control vector in

$$\mathbf{u_d} = [(\mathbf{u_d})_1 \ {\mathbf{u}_{\boldsymbol{\tau}}}^{\mathrm{T}}]^{\mathrm{T}}, \tag{15}$$

we fix the direction of $\mathbf{u}_{\boldsymbol{\tau}}$, define the corresponding feasible set, and solve the DCA problem for it. From (9) it can be shown that this set $\mathbb{U}_\tau$ of all attainable moments $\mathbf{u}_{\boldsymbol{\tau}}$ is the dodecahedron of Figure 4. This is effectively the projection of $\mathbb{U}$ onto the hyperplane $u_1 = 0$, i.e. from $\mathbb{R}^4$ to $\mathbb{R}^3$.

Remark. For quadrotors, an important advantage of the PCA over the DCA, is that it always admits a solution.

To solve the problem (5) is used to map the inequalities in (9). Then, define the normalized efforts $\tilde{u}_1 = 2\kappa_t^{-1} u_1$, $\tilde{u}_{2,3} = 2(l\kappa_t)^{-1} u_{2,3}$, and $\tilde{u}_4 = 2\kappa_d^{-1} u_4$. After some simplifications, one finds three possible values for α:

$$\begin{aligned}
\alpha_1 &= \frac{2\left(v^2_{\max} - v^2_{\min}\right)}{(l\kappa_t)^{-1}(|u_2| + |u_3|) + \kappa_d^{-1}|u_4|}, \\
\alpha_2 &= (l\kappa_t)(v^2_{\max} - v^2_{\min}) / |u_2|, \\
\alpha_3 &= (l\kappa_t)(v^2_{\max} - v^2_{\min}) / |u_3|.
\end{aligned} \tag{16}$$

The value α_1 corresponds to vectors $\mathbf{u_d}$ that intersect the regular octahedron, while α_2 and α_3 correspond to an $\mathbf{u_d}$ that intersects $\tilde{u}_2 = \pm k/2$ and $\tilde{u}_3 = \pm k/2$, respectively. Therefore, α is chosen according to the intersected face.

Solution 2 *Given α_1, α_2, and α_3 from (16), the PCA solution is*

$$\alpha = \min\{\alpha_1, \alpha_2, \alpha_3\} \tag{17}$$

that yields $\alpha\mathbf{u}_{\boldsymbol{\tau}} \in \partial\mathbb{U}_\tau$. The remaining force is left unchanged, unless it violates any of

$$\begin{aligned}
\tilde{u}_1 &\geq 8v^2_{\min} + \alpha\max\{2|\tilde{u}_2| - \tilde{u}_4,\ 2|\tilde{u}_3| + \tilde{u}_4\} \\
\tilde{u}_1 &\leq 8v^2_{\max} - \alpha\max\{2|\tilde{u}_2| + \tilde{u}_4,\ 2|\tilde{u}_3| - \tilde{u}_4\}
\end{aligned} \tag{18}$$

which is written in normalized coordinates. If (18) is violated, the force is set to the corresponding constraint value.

3.4 Suboptimal PCA (S-PCA)

Given an unattainable $\mathbf{u}_{\boldsymbol{\tau}}$, the PCA algorithm finds the maximum attainable moments vector that points in the same direction as $\mathbf{u}_{\boldsymbol{\tau}}$. However, the computation requires perfect knowledge of the elements of $\mathbf{M}$, which might be unavailable. To avoid this situation, the S-PCA, a suboptimal solution of the PCA algorithm, is proposed. This solution only requires the propellers to be balanced, and knowledge of their maximum and minimum angular velocities. Therefore, with the assumption that $\mathbf{v_d}$ is given, the solution is built without knowledge of the matrix $\mathbf{M}$ elements.

Solution 3 *Let $(\mathbf{v_c})_i = (v^2_{\max} + v^2_{\min})/2$ and*

$$\alpha = \frac{v^2_{\max} - v^2_{\min}}{2\left\|\mathbf{v_d} - \mathbf{v_c}\right\|_\infty}. \tag{19}$$

Then, the vector $\mathbf{v} = \alpha\mathbf{v_d} + (1-\alpha)\mathbf{v_c} \in \partial\mathbb{W}$.

Proof: Define the affine transformation $T(v) = v - v_c$, that shifts $\mathbb{W}$ such that $T(\mathbb{W})$ is centered on the origin. Use the DCA method to find the optimum $\alpha T(\mathbf{v_d}) \in \partial T(\mathbb{W})$, with α from (19). Shift this solution back to $\mathbb{W}$, yielding $\mathbf{v} = T^{-1}(\alpha T(\mathbf{v_d})) = \alpha\mathbf{v_d} + (1-\alpha)\mathbf{v_c}$. Since the described transform is homeomorphic, $\partial T(\mathbb{W})$ is mapped back to $\partial\mathbb{W}$, and the solution cannot be further optimized. □

Proposition 1 *The vector* $\mathbf{v} = \alpha\mathbf{v_d} + (1-\alpha)\mathbf{v_c}$ *is a suboptimal solution of the PCA method that preserves the desired moments vector direction.*

Proof: From (5), for an equal velocity among the propellers no torque is produced. Therefore,

$$\mathbf{u} = \mathbf{M}\mathbf{v} = \alpha\mathbf{u_d} + \begin{bmatrix} * & 0 & 0 & 0 \end{bmatrix}^{\mathrm{T}}, \qquad (20)$$

which shows that the desired torque vector is scaled according to $\alpha\mathbf{u_\tau}$. Hence, its direction is preserved. To prove that the $\mathbf{u} = \alpha\mathbf{u_d}$ might be suboptimal, note that $\mathbf{v} \in \partial\mathbb{W} \iff \mathbf{u} \in \partial\mathbb{U}$. However, $\mathbf{u} \in \partial\mathbb{U} \not\Longrightarrow \alpha\mathbf{u_\tau} \in \partial\mathbb{U}_\tau$, since points on $\partial\mathbb{U}$ are mapped in the interior $\mathrm{int}(\mathbb{U}_\tau)$ of $\mathbb{U}_\tau$. Therefore, $\exists\mathbf{u_d}$ such that $\mathbf{u} \in \partial\mathbb{U}$ but $\alpha\mathbf{u_\tau} \in \mathrm{int}(\mathbb{U}_\tau) \iff \alpha\mathbf{u_\tau} \notin \partial\mathbb{U}_\tau$. □

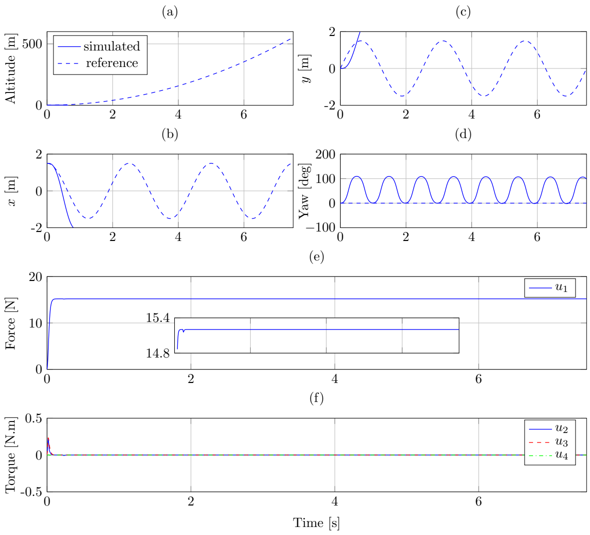

Figure 5: Unmanaged rotors saturation. (a) to (c) vehicle position; (d) yaw angle; (e) required thrust force and (f) required torques.

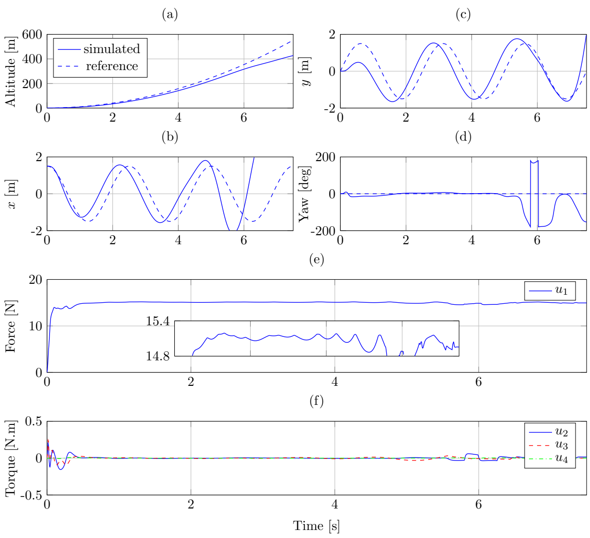

Figure 6: Simulation results for the DCA.

4 Simulation Results

The previous results are validated in MATLAB with an Ascending Technologies Hummingbird model (Mueller and D'Andrea, 2014) that includes drag and first order motor dynamics with time constant 0.015 s. From this model the saturation levels are computed, yielding

$$178 \text{ rad/s} \le v_i \le 770 \text{ rad/s}, \ \forall i. \qquad (21)$$

This implies the following propellers thrust force:

$$0.2 \text{ N} \le f_i \le 3.8 \text{ N}, \ \forall i. \qquad (22)$$

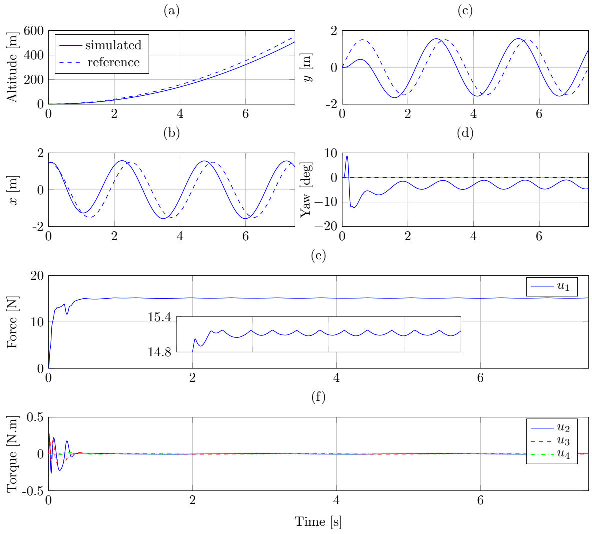

Figure 7: Simulation results for the PCA.

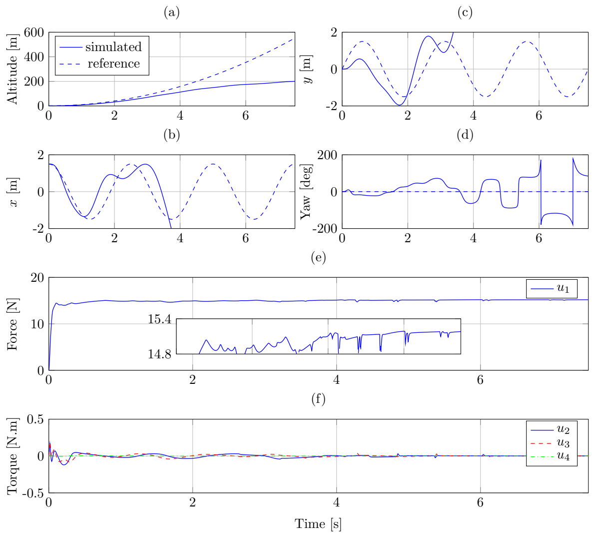

Figure 8: Simulation results for the S-PCA.

A high-level cascaded controller is implemented, following the PD and Backstepping used in (Monteiro et al., 2016). The controller consists of a PD outer loop that controls the position, while the inner loop controls the attitude of the vehicle through the Backstepping technique (Bouabdallah, 2007).

To evaluate the methods the quadrotor is required to ascend with $2g$ acceleration, i.e. along $-\overrightarrow{\mathbf{z_e}}$, hold a fixed yaw angle, and describe a circle of radius $1.5m$ on the xy-plane. The objective of this simulation is to force the vehicle to work near its saturation levels. Similar situations occur when the quadrotor needs to carry a heavy load, since this scenario also requires the motors to produce more thrust.

4.1 Discussion

If one considers the whole simulation, the vehicle stability is guaranteed only when the PCA strategy is used. None of the other algorithms were capable of achieving this performance. Nonetheless, both the DCA and S-PCA, which does not depend directly one **M**, maintained the stability for a limited time. Comparing these two, the DCA method showed a better overall performance, that degraded only after 5 s. At this point the vehicle had already achieved 200 m. Therefore, depending on the duration of the prescribed maneuver, this could be satisfactory. The case depicted in Figure 5 represents the case where no control allocation strategy is used and the propellers saturates arbitrarily. This is evidently the worst performance, and the vehicle was not able to follow the trajectory at all.

5 Conclusion

This work studied four control allocation strategies, which regard control bound constraints. These strategies were tested via simulations on a quadrotor UAV model. The first strategy was a reformulation of the WLS allocation as a QP problem. The motivation for this was to reduce computational cost, which favors real-time implementation on embedded systems. Secondly, a simple solution to the DCA method was deduced. However simple, we showed that this solution might not exist. Then, the PCA method and its solution were restated. Besides generating higher torques, the solution was proved to exist for every desired control effort. Noticing that the exact knowledge of the matrix **M** elements, required for the PCA solution, might be unavailable, we proposed the S-PCA strategy. The solution obtained through the S-PCA is suboptimal when compared to that of the PCA, but it does not require this previous knowledge.

It is worth noting that some other simulations scenarios, with different flight conditions, favored the DCA over the PCA strategy. This indicates that the situations that might benefit one over the other need further investigation.

All but the QP strategy were evaluated via simulation. The case where no explicit control allocation strategy is employed, and therefore saturation is not managed, stressed the importance of control allocation. Applying any of the other methods improved the performance significantly. The unstable response observed using the DCA strategy might be due to its lower attainable torque, when compared to the PCA. Therefore, a study on which flight situations result in the unsolvability of the DCA scheme is still necessary.

References

Bouabdallah, S. (2007). *Design and control of quadrotors with application to autonomous flying*, PhD thesis, École Polytechnique Federale de Lausanne.

Ducard, G. and Hua, M.-D. (2011). Discussion and practical aspects on control allocation for a multi-rotor helicopter, *Int. Conf. on Unmanned Aerial Vehicle in Geomatics*.

Durham, W. C. (1993). Constrained control allocation, *J. of Guidance, Control, and Dyn.* **16**(4): 717–725.

Härkegård, O. (2002). Efficient active set algorithms for solving constrained least squares problems in aircraft control allocation, *IEEE Conf. on Dec. and Contr.*, Vol. 2, IEEE, pp. 1295–1300.

Johansen, T. A. and Fossen, T. I. (2013). Control allocation – a survey, *Automatica* **49**(5): 1087–1103.

Marks, A., Whidborne, J. F. and Yamamoto, I. (2012). Control allocation for fault tolerant control of a VTOL octorotor, *UKACC Int. Conf. on Control*, IEEE, pp. 357–362.

Mellinger, D. and Kumar, V. (2011). Minimum snap trajectory generation and control for quadrotors, *IEEE Int. Conf. on Robot. and Autom.*, pp. 2520–2525.

Mellinger, D., Michael, N. and Kumar, V. (2012). Trajectory generation and control for precise aggressive maneuvers with quadrotors, *Int. J. of Robot. Research* **31**(5).

Monteiro, J. C., Lizarralde, F. and Hsu, L. (2016). Optimal control allocation of quadrotor UAVs subject to actuator constraints, *American Contr. Conf.*, IEEE.

Mueller, M. W. and D'Andrea, R. (2014). Stability and control of a quadrocopter despite the complete loss of one, two, or three propellers, *IEEE Int. Conf. on Robot. and Autom.*, pp. 45–52.

Petersen, J. A. and Bodson, M. (2006). Constrained quadratic programming techniques for control allocation, *IEEE Trans. on Control Syst. Tech.* **14**(1): 91–98.

Yoon, H.-J., Cichella, V. and Hovakimyan, N. (2016). Robust adaptive control allocation for an octocopter under actuator faults, *AIAA Guidance, Navigation., Control, Conf.*, p. 0635.

ISSN 2525-8311